J Wood Sci (2015) 61:608–619
DOI 10.1007/s10086-015-1513-8

ORIGINAL ARTICLE

Enzymatic dehydrogenative polymerization of monolignol dimers

Yasuyuki Matsushita[1] · Chisato Ko[1] · Dan Aoki[1] · Shota Hashigaya[1] · Sachie Yagami[1] · Kazuhiko Fukushima[1]

Received: 9 June 2015 / Accepted: 27 August 2015 / Published online: 19 September 2015

Abstract The structure and biosynthesis of lignin are not yet fully understood, especially the step following the initial dimerization of monolignol. Liquid chromatograph mass spectrometer (LC–MS) was used to analyze the consumption rates of monolignol dimers formed by β-*O*-4, β-5, and β-β couplings between coniferyl alcohols in efforts to understand the activity of monolignol dimers in enzymatic dehydrogenative polymerization. We investigated the reaction kinetics in single-component and mixed-component reaction systems containing one and two species of the dimers, respectively. A difference was observed between the consumption rates of the three dimers we tested, and the consumption rate of one dimer in the single-component reaction was different from that in a mixed-component reaction. In qualitative LC–MS analyses, coniferyl alcohol oligomers were detected in the reaction products. Some monolignol tetramers were formed by 5-5 and 5-*O*-4 coupling between the dimers. The results of this work suggested that monolignol dimers with β-5 and β-β linkages could function as radical mediators in enzyme-catalyzed polymerization.

Keywords Enzymatic dehydrogenative polymerization · Lignification · Monolignol · Dimer · Reaction kinetics

Introduction

Lignin, along with cellulose and hemicellulose, is one of the major components of wood [1]. In plant cell walls, lignin within cellulose microfibrils performs several important functions for the plant body [2], such as mechanical support [3–5] and disease resistance [6–8]. The main lignin precursors are the three hydroxycinnamyl alcohols (termed monolignols): *p*-coumaryl alcohol, coniferyl alcohol, and sinapyl alcohol. The heterogeneous structure of lignin is formed by complicated dehydrogenative polymerizations of these monolignols, with specific combinations and relative abundances of the monomers being dependent on the plant types. For example, dicotyledonous angiosperm lignin is derived from coniferyl and sinapyl alcohols with a trace amount of *p*-coumaryl alcohol, whereas gymnosperm lignin is generated from coniferyl alcohol and a small amount of *p*-coumaryl alcohol. Grass lignin is made of coniferyl, sinapyl, and *p*-coumaryl alcohols [1]. Despite its importance in wood cells, the structure and biosynthesis of lignin are not yet fully understood. Therefore, for our further understanding of the structure and formation of lignin, this work seeks to elucidate how macromolecular lignin is synthesized from monolignols.

Studies of the biosynthesis and structure of lignin have been carried out by the in vitro enzymatic dehydrogenative polymerization of monolignols. In lignin biosynthesis, monolignols are formed in the cytosol, transported to cell walls, and then undergo one-electron oxidation catalyzed by enzymes such as peroxidase or laccase [9, 10]. Since peroxidases are known to be common enzymes for lignification [11], a commercially available enzyme, horseradish peroxidase (HRP), is often used for in vitro reactions [12–14]. The first step in the formation of lignin is the

Part of this paper was presented at the 58th Lignin Symposium (Kagawa, Japan, 2013), the International Conference on Polyphenols (Nagoya, Japan, 2014), and the International Symposium on Wood Science and Technology (Tokyo, Japan, 2015).

✉ Yasuyuki Matsushita
ysmatsu@agr.nagoya-u.ac.jp

[1] Graduate School of Bioagricultural Sciences, Nagoya University, Nagoya 464-8601, Japan

generation of two free radicals from a mixture of monolignols by enzyme-catalyzed oxidation, followed by coupling to form a dimer. The dimer then undergoes radical coupling with a monolignol, another dimer, or an oligomer. This radial coupling propagates to construct lignin. There are many reports on the dimerization and polymerization of monolignols [10, 13–16]. However, the specific behavior of monolignol dimers during enzymatic dehydrogenative polymerization has not been investigated in any detail. What we do know is the following. Two modes of lignification—"end-wise" and "bulk"—are widely known [17, 18]. The former is a reaction between a monolignol and a monolignol oligomer, and the latter is a reaction between two monolignol oligomers. Currently, the former mode is regarded as the predominant process in lignin formation [19, 20]. However, the reaction rate of enzymatic oxidation of monolignols is far higher than that of dimers, which leads to a large abundance of dimers in the initial stage of lignification. Therefore, coupling/cross-coupling between dimers can occur frequently.

The aim of this study is to investigate the reaction kinetics of monolignol dimers to understand lignin formation in its initial stage. Three major dimers [21, 22], guaiacylglycerol-β-coniferyl ether (**I**), dehydrodiconiferyl alcohol (**II**), and pinoresinol (**III**), which contain β-*O*-4, β-5, and β-β linkages, respectively, were used (Fig. 1).

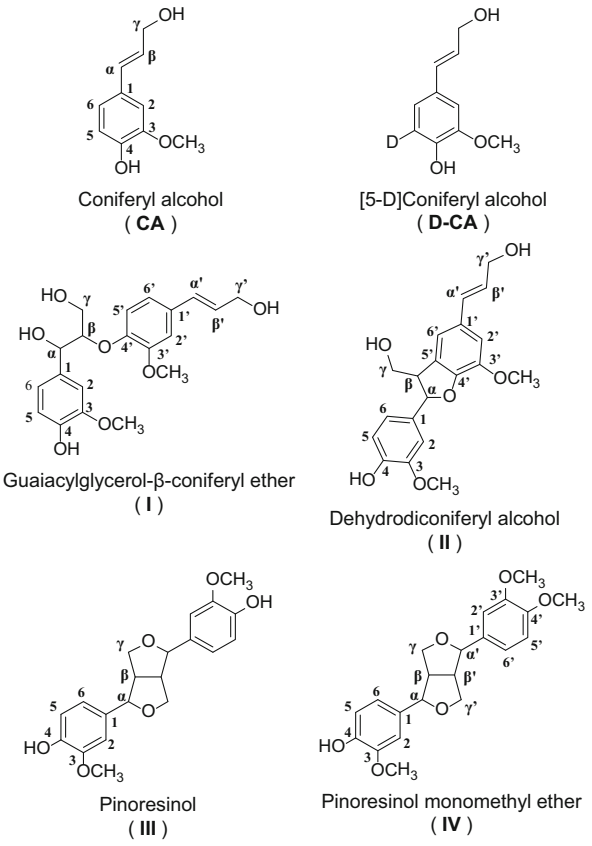

Fig. 1 Chemical structures of the compounds used in this study

Materials and methods

Preparation of coniferyl alcohol and [5-D]coniferyl alcohol

Coniferyl alcohol (**CA**) was prepared according to previously described methods [21]. [5-D]vanillin was synthesized using deuterium oxide according to a previously published procedure [23]. Condensation of the deuterium-labeled vanillin with monoethyl malonate followed by reduction using lithium aluminum hydride gave [5-D]-coniferyl alcohol (**D-CA**) [21].

Preparation of monolignol dimers

Coniferyl alcohol was subjected to an oxidative coupling reaction using silver (I) oxide to obtain monolignol dimers [24]. Three monolignol dimers were produced: guaiacylglycerol-β-coniferyl ether (**I**), dehydrodiconiferyl alcohol (**II**), and pinoresinol (**III**). These three dimers were isolated by flash column chromatography (Agilent 971-FP, Agilent Technologies) using a silica gel column (Super Flash SF, Agilent Technologies) and a mixture of benzene and ethyl acetate as the eluent. The synthesis of **I** produced diastereomers. The erythro/threo ratio for **I** was 0.8, according to the intensity of peaks at the β position in the ^{13}C NMR spectrum (erythro: 86.56 ppm, threo: 88.26 ppm). [5-D]coniferyl alcohol dimers (**D-I**, **D-II**, and **D-III**) were synthesized using **D-CA** by the same method.

I: ^{1}H NMR (in acetone-d$_6$) δ: 3.50 (1H, dd, $J = 5.6$, 12.0 Hz, H-γ1), 3.70 (1H, dd, $J = 3.2$, 12.0 Hz, H-γ2), 3.81 (3H, s, 3-OCH$_3$), 3.85 (3H, s, 3′-OCH$_3$, *erythro* isomer), 3.89 (3H, s, 3′-OCH$_3$, *threo* isomer), 4.22 (1H, m, H-β), 4.31 (2H, dd, $J = 5.4$, 1.6 Hz, H-γ′), 4.90 (1H, br d, $J = 5.2$, 6.0 Hz, H-α, *threo* isomer), 4.90 (1H, br d, $J = 5.2$, 6.0 Hz, H-α, *erythro* isomer), 6.28 (1H, dt, $J = 15.8$, 5.4 Hz, H-β′, *erythro* isomer), 6.30 (1H, dt, $J = 15.8$, 5.4 Hz, H-β′, *threo* isomer), 6.52 (1H, dt, $J = 15.8$, 1.6 Hz, H-α′, *erythro* isomer), 6.54 (1H, dt, $J = 15.8$, 1.6 Hz, H-α′, *threo* isomer), 6.77 (1H, d, $J = 8.0$ Hz, H-5, *erythro* isomer), 6.78 (1H, d, $J = 8.0$ Hz, H-5, *threo* isomer), 6.86 (1H, d, $J = 2.0$ Hz, H-2, *threo* isomer), 6.88–6.90 (1H, m, H-6), 6.93 (1H, d, $J = 6.0$ Hz, H-5′, *erythro* isomer), 7.05 (1H, d, $J = 2.0$ Hz, H-2, *erythro* isomer), 7.09 (1H, d, $J = 1.6$ Hz, H-2′), 7.12 (1H, d, $J = 6.0$ Hz, H-5′, *threo* isomer); ^{13}C NMR δ: 56.18, 56.20, 56.31, 61.81, 61.86, 63.26, 73.79, 73.81, 86.56, 88.26, 110.82, 110.96, 111.39, 115.15, 115.23, 119.20, 119.48, 120.24, 120.32, 120.44, 120.52, 129.47, 129.57, 129.88,

129.90, 132.80, 132.91, 133.77, 134.19, 146.63, 146.81, 147.96, 148.02, 148.50, 149.09, 151.63, 151.81.

II: ^{1}H NMR (in acetone-d_6) δ: 3.54 (1H, q, $J = 6.4$ Hz, H-β), 3.81–3.91 (2H, m, H-γ), 3.82 (3H, s, 3-OCH_3), 3.86 (3H, s, 3′-OCH_3), 4.20 (2H, d, $J = 5.6$ Hz, H-γ′), 5.57 (1H, d, $J = 6.4$ Hz, H-α), 6.24 (1H, dt, $J = 16.0$ Hz, 5.6 Hz, H-β′), 6.53 (1H, d, $J = 16.0$ Hz, H-α′), 6.81 (1H, d, $J = 8.0$ Hz, H-5), 6.89 (1H, dd, $J = 2.0$ Hz, 8.0 Hz, H-6), 6.95 (1H, s, H-2′), 6.98 (1H, s, H-6′), 7.04 (1H, d, $J = 2.0$ Hz, H-2); ^{13}C NMR δ: 56.28, 56.39, 54.78, 63.41, 64.63, 88.54, 110.50, 111.72, 115.70, 116.10, 119.59, 128.37, 130.42, 130.56, 131.94, 134.38, 145.18, 147.31, 148.40, 148.97.

III: ^{1}H NMR (in acetone-d_6) δ: 3.09 (2H, m, H-β), 3.81 (2H, dd, $J = 3.6$ Hz, 8.8 Hz, H-γ1), 3.84 (6H, s, 3-OCH_3), 4.20 (2H, dd, $J = 6.8$ Hz, 8.8 Hz, H-γ2), 4.67 (2H, d, $J = 4.0$ Hz, H-α), 6.79 (2H, d, $J = 8.0$ Hz, H-5), 6.84 (2H, dd, $J = 1.6$ Hz, 8.0 Hz, H-6), 6.99 (2H, d, $J = 1.6$ Hz, H-2); ^{13}C NMR δ: 55.24, 56.26, 72.22, 86.65, 110.63, 115.56, 119.62, 134.16, 146.90, 148.36.

Preparation of pinoresinol monomethyl ether (IV)

Here, **III** (0.14 mmol) was dissolved in *N*,*N*-dimethylformamide (5 mL). Potassium carbonate (0.084 mmol) and iodomethane (0.14 mmol) were added, and then the mixture was stirred in an oil bath at 60 °C. After 1.5 h, the progress of the reaction was checked by thin-layer chromatography (TLC). More iodomethane (0.14 mmol) was added if the reaction was not complete. In our synthesis, 0.56 mmol of additional iodomethane was added. After the reaction, dilute hydrochloric acid was added until the pH of the mixture was adjusted to ~3. The solution was then extracted three times using ethyl acetate, and then washed with distilled water four times, and finally once by saturated salt water. The extract was dried by anhydrous sodium sulfate, and the solvent was evaporated. The product, **IV**, was purified by preparative TLC (yield 35.5 %).

IV: ^{1}H NMR (in acetone-d_6) δ: 3.09 (2H, m, H-β and H-β'), 3.79 (3H, s, 4′-OCH_3), 3.81 (3H, s, 3′-OCH_3), 3.82 (2H, dd, $J = 6.9$ Hz, 8.9 Hz, H-γ1 and H-γ′1), 3.85 (3H, s, 3-OCH_3), 4.21 (2H, dd, $J = 6.9$ Hz, 8.9 Hz, H-γ2 and H-γ′2), 4.68 (1H, d, $J = 4.2$ Hz, H-α), 4.70 (1H, d, $J = 4.2$ Hz, H-α′), 6.79 (2H, d, $J = 8.1$ Hz, H-5 and H-5′), 6.84 (2H, dd, $J = 1.8$ Hz, 8.1 Hz, H-6, and H-6′), 6.91 (1H, d, $J = 1.8$ Hz, H-2′), 7.00 (1H, d, $J = 1.8$ Hz, H-2); ^{13}C NMR δ: 55.25, 55.27, 56.09, 56.16, 56.26, 72.23, 72.29, 86.51, 86.64, 110.62, 111.00, 112.64, 115.56, 119.09, 119.63, 134.17, 135.43, 146.90, 148.36, 149.81, 150.46.

Enzyme activity

In this study, HRP (Wako Pure Chemical Industries) was used as the enzyme for dehydrogenative polymerization of **CA** and monolignol dimers. In order to measure the activity of HRP, a 20 mM solution of guaiacol (50 μL) was mixed with 6 mM hydrogen peroxide (50 μL) and distilled water (2.95 mL). After addition of 2.0 μg/mL HRP solution (50 μL), the absorbance of the mixture at 436 nm was measured with an ultraviolet–visible absorption spectrophotometer (V-530, JASCO). The enzyme activity was calculated according to a following Eq. (1) and estimated to be 87.5 units/mg.

$$A = \frac{(\Delta E_s - \Delta E_b) \times 4 \times 3.1}{K \times 2.0 \times 10^{-3} \times 0.05} \quad (1)$$

where A is the enzyme activity (units/mg), ΔE_s is the increasing rate (per min) of the absorbance of the reaction solution between 5 and 10 min after HRP addition, ΔE_b is the absorbance of the blank solution (without HRP addition), K is 25.5, which is the molar absorption coefficient of tetraguaiacol.

Enzymatic dehydrogenative polymerization

In this study, two systems were employed, a single-component system and a mixed-component system. Their preparation is described in the following sections.

Single-component reaction

A monolignol dimer (**I**, **II**, or **III**), or **CA** was used as the substrate for the single-component dehydrogenative polymerization reaction catalyzed by HRP. A mixture of the substrate (0.015 mmol) in 1 mL of acetone and 73 mL of distilled water was prepared and stirred at 700 rpm. A 0.01 mg/mL solution of HRP in distilled water (1 mL) and 0.005 % hydrogen peroxide solution (25 mL) were added to the substrate solution while stirring. At a given time, a 3-mL aliquot of the reaction solution was removed and mixed with 1 mL of a 0.01 mg/mL distilled water solution of catalase to stop the enzymatic reaction. The resulting product was freeze-dried, extracted with methanol, and membrane-filtrated (PTFE 0.50 μm, DISMIC-13JP, ADVANTEC) for LC–MS analysis. The experiments were performed in triplicate.

Mixed-component reaction

A mixture of two different monolignol dimers (**I** + **II**, **I** + **III**, and **II** + **III**; 0.5:0.5, mol/mol) was used to investigate mixed-component dehydrogenative polymerization reactions catalyzed by HRP. The dehydrogenative polymerization and sampling were conducted by the same method as that described above for the single-component reaction. The experiments were performed in triplicate.

LC–MS analysis

The samples obtained from the single-component and mixed-component dehydrogenative polymerization reactions were analyzed by LC–MS. The apparatus consisted of an LC system (DGU-20A$_3$/LC-20AD/CBM-20A/SIL-20AC/SPD-20A/CTO-20A, SHIMADZU, Japan) fitted with a Luna 5u Phenyl-Hexyl 150 mm × 2.0 mm column (Phenomenex, USA), and an MS system (API2000, AB SCIEX, USA). Electrospray ionization and positive ion mode were used in this study. The mobile phase consisted of 1 mM trifluoroacetic acid (TFA) in ultrapure water (solvent A, later referred to as A) and a mixture of methanol and acetonitrile (6:1, v/v) (solvent B, later referred to as B). The flow rate was set to 0.2 mL/min, and the temperature of the column was set to 40 °C. A UV detection wavelength of 280 nm was selected because guaiacyl lignin compounds derived from CA typically show a UV absorption maximum at 280 nm [25]. The data were analyzed using the Analyst 1.6.1 software package (AB SCIEX, USA).

For the quantitative analyses of monolignol dimers in the reaction solutions, the elution gradient was 0–4 min, 20 % B; 4–10 min, linear gradient from 20 to 30 % B, 10–15 min, 30 % B; 15–40 min, linear gradient from 30 to 50 % B; 40–80 min, linear gradient from 50 to 60 % B; 80–85 min, 60 % B; 85–90 min, linear gradient from 60 to 20 % B. The amounts of the monolignol dimers in the solutions were determined by UV absorption.

For the qualitative analyses of the enzymatic dehydrogenative polymerization products derived from the monolignol dimers, the elution gradient was 0–8 min, 20 % B; 8–20 min, linear gradient from 20 to 30 % B; 20–30 min, 30 % B; 30–80 min, linear gradient from 30 to 50 % B; 80–160 min, linear gradient from 50 to 60 % B; 160–170 min, 60 % B; 170–180 min, linear gradient from 60 to 20 % B. The monolignol oligomers were detected by LC–MS. The MS parameters were configured as follows: curtain gas, 20; ion spray voltage, 5500 V; temperature, 400 °C; ion source gas 1, 70; ion source gas 2, 80; interface heater, ON.

Cyclic voltammetry analysis

A monolignol dimer or **CA** (0.025 mmol) was dissolved in 8 mL of a mixture of acetone and distilled water (3:1, v/v). The solution's oxidation potential was determined by cyclic voltammetry (CV). The CVs were recorded using an Automatic Polarization System (HZ-7000, Hokuto Denko, Japan) connected to a personal computer. The counter electrode was a Pt wire. A Ag/AgCl electrode connected to a saturated KCl solution using a salt bridge was used as the reference electrode, and a Pt disk (diameter 1.6 mm) was used as the working electrode. Prior to the experiment, the working electrode was polished with a slurry containing 0.05-μm alumina particles and then rinsed with distilled water. The scan rate was 100 mV/s. The experiments were performed in triplicate.

Results

Consumption rates of monolignol dimers

The results of the quantitative analyses of the residual ratio of substrates in the single-component dehydrogenative polymerization reactions (Fig. 2) show that the order of consumption rates was **III** > **II** > **I**. Figure 3 shows the results of the quantitative analyses for the mixed-component reactions. In the mixed-component reactions containing **I**, i.e., the mixed-component reactions of **I** + **II** and **I** + **III**, the consumption rate of **I** increased, and those of **II** and **III** decreased compared with the single-component reactions. In the mixed-component reaction of **II** + **III**, the consumption rate of **II** decreased and that of **III** increased slightly compared with the single-component reactions.

Oxidation potentials of monolignol dimers

The oxidation potentials of the monolignol dimers (**I**, **II**, and **III**) obtained from CV analyses are reported in Table 1. There was no significant difference between the three dimers according to the results of the *t* test. From these results, it is clear that all three dimers have similar oxidation potentials.

Qualitative analyses of reaction products

Monolignol oligomers, i.e., tetramers, hexamers, and octamers, formed by radical coupling between monolignol

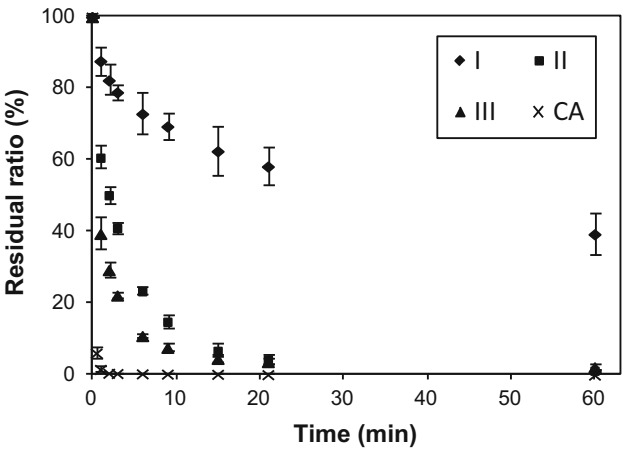

Fig. 2 The time course of residual ratio of **CA** and the monolignol dimers in the single-component reactions

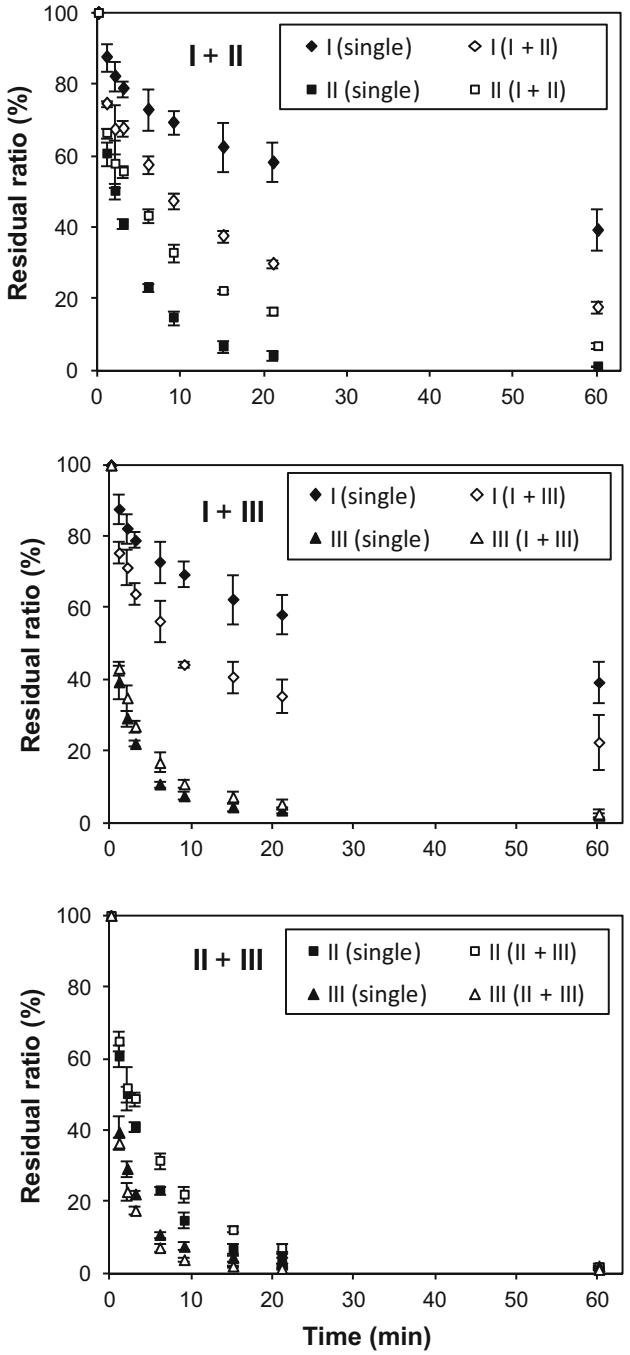

Fig. 3 The time course of residual ratio of the monolignol dimers in the mixed-component reactions. Those in the single-component reactions were each described on a same figure for reference

dimers, were detected in the total ion chromatograms obtained from the LC–MS analyses. Several monolignol tetramers derived from the single-component reactions were identified by comparing the mass spectra of monolignol tetramers obtained from unlabeled dimers with those from deuterium-labeled dimers. The molecular weight of **D-CA** increased by 1 relative to **CA**, which led to the molecular weights of **D-I** and **D-III** being 2 higher than those of **I** and **III**, and the molecular weight of **D-II** being 1 higher than that of **II**. When a deuterium-labeled tetramer was generated from radical coupling of two deuterium-labeled dimers via the 5-positions (5-5 linkage), the molecular weight of the tetramer from **D-II** was equal to that from **II**, whereas those from **D-I** and **D-III** were 2 higher than **I** and **III**, respectively. By contrast, when radical coupling occurs between the 5-position and the phenolic oxygen (5-*O*-4 linkage), the molecular weight of the deuterium-labeled tetramer from **D-II** increased by 1 relative to that of an analog synthesized from **II**, while the molecular weights of the tetramer derived from **D-I** and **D-III** increased by 3 relative to those of **I** and **III**, respectively.

Table 1 Oxidation potentials of coniferyl alcohol (CA) and the monolignol dimers by cyclic voltammetry (CV)

	Oxidation potential (mV)
CA	170 ± 19.6
I	251 ± 23.8
II	279 ± 11.1
III	253 ± 21.3
IV	267 ± 12.0

Mean value ± standard error

LC–MS chromatograms of the products from the single-component reaction of **I** are shown in Fig. 4. In this figure, the *m*/*z* range for chromatogram (A) was set to 710–780 to detect monolignol tetramers derived from **I**, and the *m*/*z* range for chromatogram (B) was set to 1084–1154 to detect monolignol hexamers derived from **I**. In Fig. 4a, two peak groups for monolignol tetramers were detected. These tetramers were identified by comparison with mass spectra obtained from reactions using **I** and **D-I**. The peaks in the group at 42.6–49.0 and 51.2–55.3 min were assigned to tetramers from two **I**s connected via 5-5 [**I**(5-5)**I**] and 5-*O*-4 [**I**(5-*O*-4)**I**] linkages, respectively. These assignments were made because the molecular weights of the tetramers derived from **D-I** increased by 2 and 3, respectively, compared with the tetramers obtained from **I**. Additionally, **I** has enantiomeric and diastereomeric centers, which led to the generation of a variety of diastereomers in **I**(5-5)**I** and **I**(5-*O*-4)**I**. Figure 4b show that hexamers were also generated in the single-component reaction using **I**.

Figure 5 shows the total ion chromatograms of the single-component reaction products of **II**. In this figure, the *m*/*z* range for chromatogram (A) was set to 674–744 to detect the monolignol tetramers derived from **II**, the *m*/*z* range for chromatogram (B) was set to 1030–1100 in order to detect the monolignol hexamers derived from **II**, and the *m*/*z* range for chromatogram (C) was set to 1386–1456 in order to detect the monolignol octamers derived from **II**. In Fig. 5a, peaks appearing at 75.8 and 81.8 min were assigned to tetramers linked via the 5-5 [**II**(5-5)**II**] and

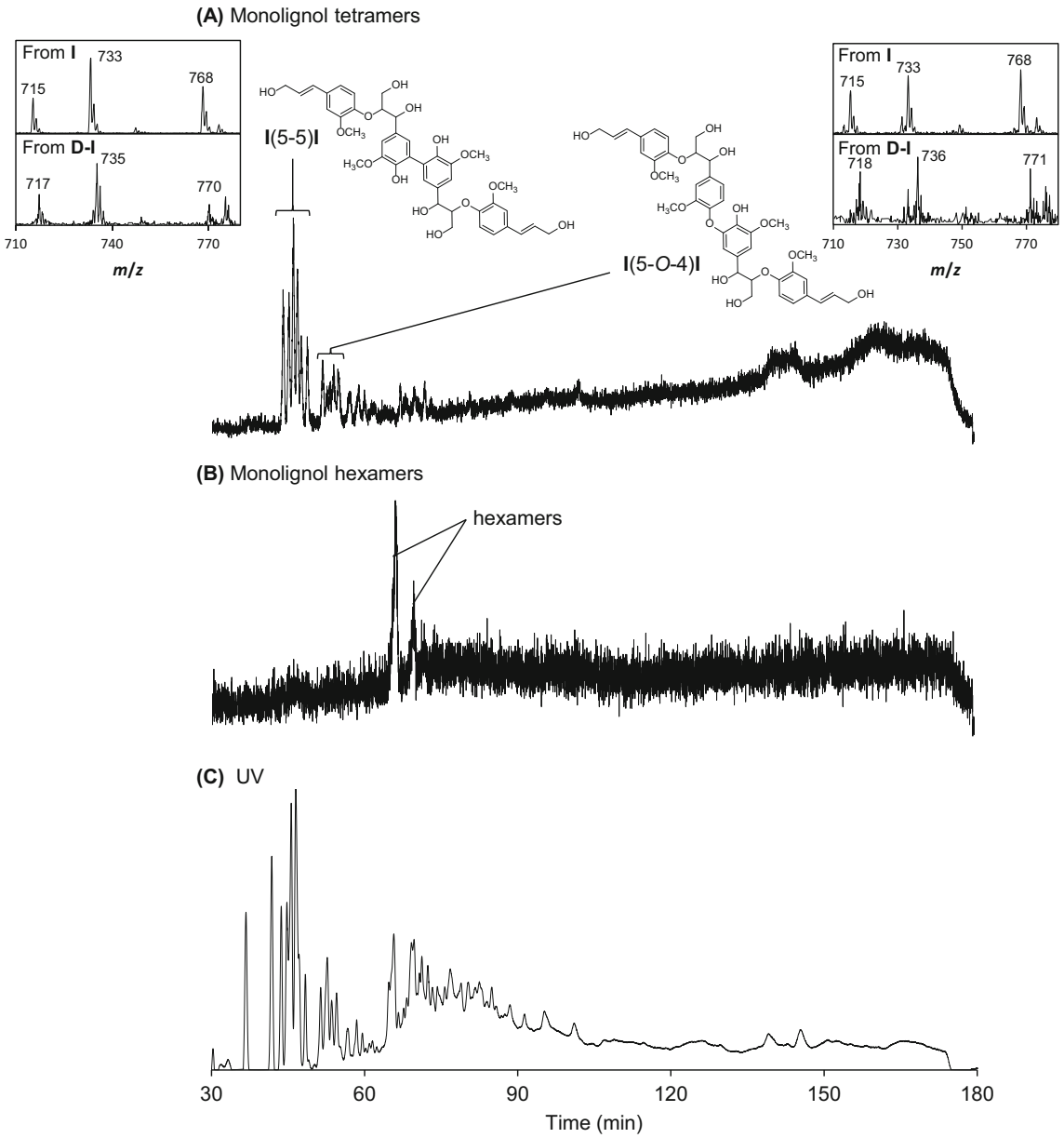

Fig. 4 Total ion chromatograms and UV chromatogram of the single-component reaction products from **I**. Scanning ranges were (**a**) *m*/*z* 710–780 and (**b**) *m*/*z* 1084–1154, according to assumed *m*/*z* of monolignol tetramers and hexamers derived from **I**. Mass spectra of the monolignol tetramers derived from **I** and **D-I** are also described

5-*O*-4 [**II**(5-*O*-4)**II**] linkages, respectively, in the same manner as described above, except that the increase in the molecular weight of the tetramers derived from **D-II** was 0 and 1, respectively, compared with those of the tetramers from **II**. Figure 5b, c show that octamers and hexamers are generated in the single-component reaction using **II**.

The total ion chromatograms of the single-component reaction products from **III** are shown in Fig. 6. In this figure, the *m*/*z* range for chromatogram (A) was set to 674–744 to detect the monolignol tetramers derived from **III**, and the *m*/*z* range for chromatogram (B) was set to 1030–1100 to detect the monolignol hexamers derived from **III**. In Fig. 6a, two peaks at 101.6 and 114.9 min were assigned to tetramers linked via the 5-5 [**III**(5-5)**III**] and 5-*O*-4 [**III**(5-*O*-4)**III**] linkages, respectively, using the same analysis method described in the previous paragraph. The molecular weights of the tetramers from **D-III** were 2 and 3 higher than those from **III,** respectively. Figure 6b shows that hexamers are also generated from the single-component reaction using **III**.

The reaction products from the mixed-component reactions were investigated by LC–MS. In LC

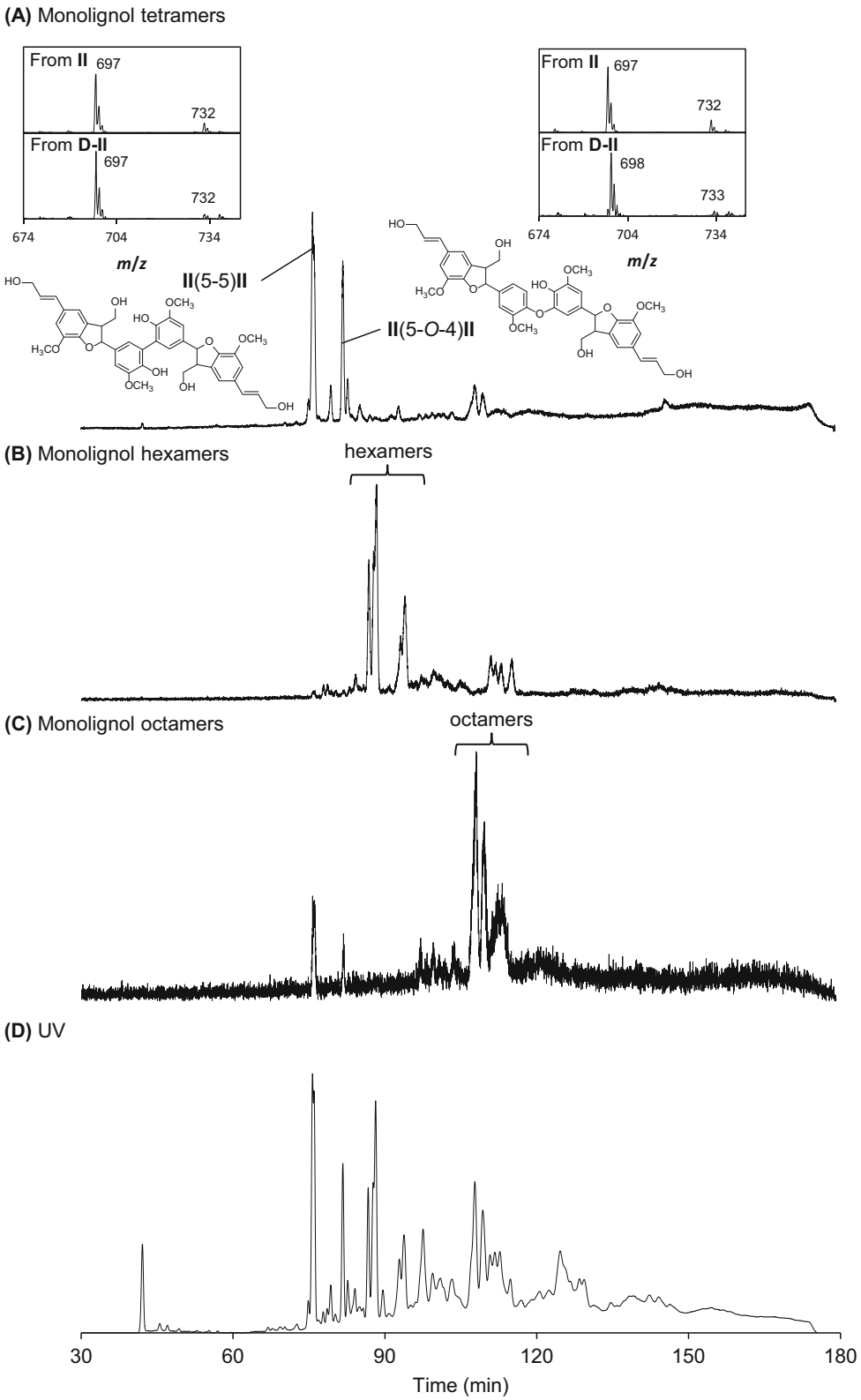

Fig. 5 Total ion chromatograms and UV chromatogram of the single-component reaction products from **II**. Scanning ranges were (**a**) *m/z* 674–744, (**b**) *m/z* 1030–1100, and (**c**) *m/z* 1386–1456, according to assumed *m/z* of monolignol tetramers, hexamers, and octamers derived from **II**. Mass spectra of the monolignol tetramers derived from **II** and **D-II** are also described

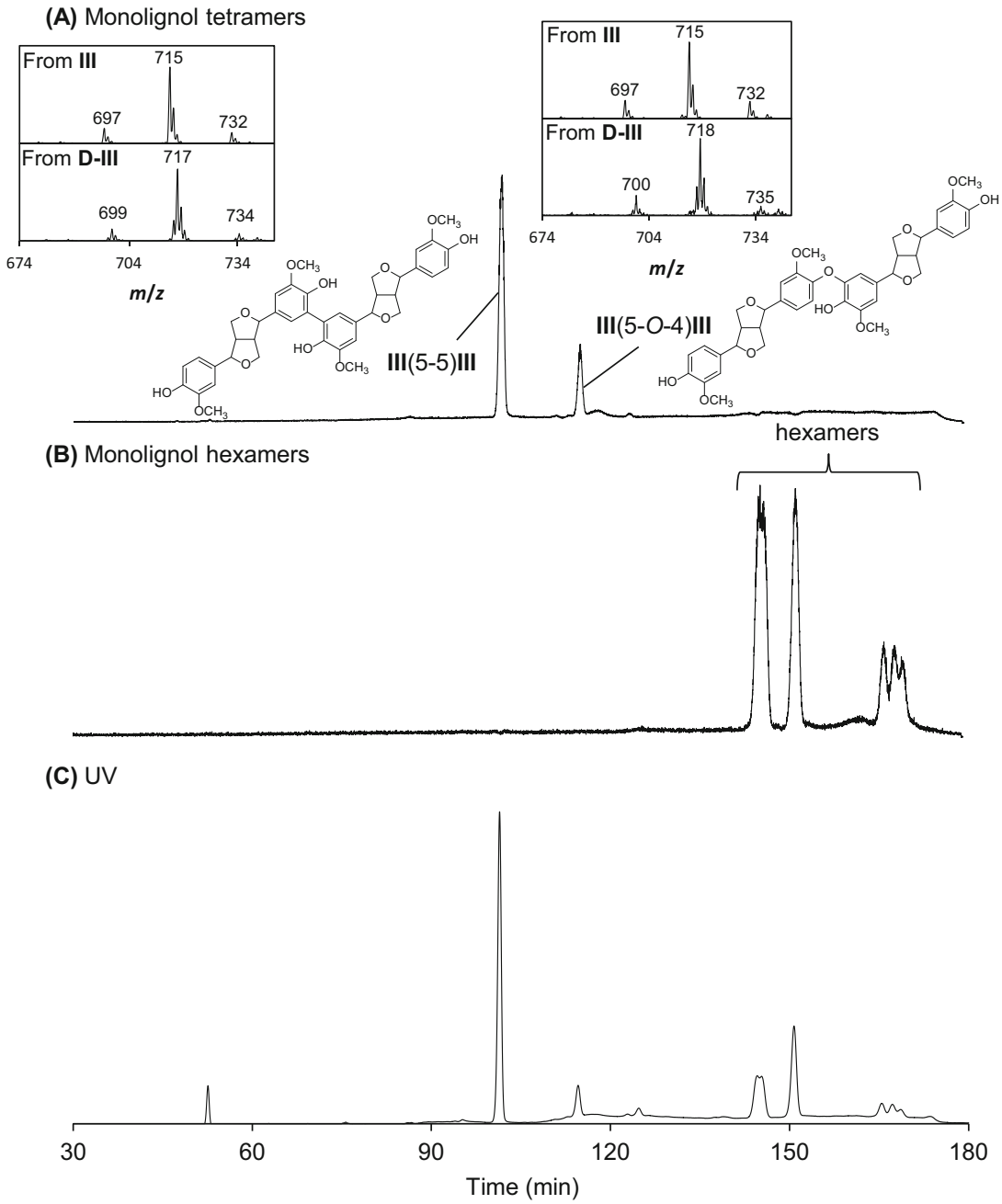

Fig. 6 Total ion chromatograms and UV chromatogram of the single-component reaction products from **III**. Scanning ranges were (**a**) *m*/*z* 674–744 and (**b**) *m*/*z* 1030–1100, according to assumed *m*/*z* of monolignol tetramers and hexamers derived from **III**. Mass spectra of the monolignol tetramers derived from **III** and **D-III** are also described

chromatograms obtained for the mixed-component reactions, peaks corresponding to the single-component reaction products were detected, and some peaks were also detected that were not detected in the single-component reactions. This result shows that monolignol oligomers derived from the radical couplings of different types of monolignol dimers were formed during the mixed-component reactions.

Discussion

Consumption rates of monolignol dimers in single-component reactions

In the dehydrogenative polymerization of monolignol dimers catalyzed by HRP, a radical of a monolignol dimer was generated by association between the active site of

HRP and the phenolic hydroxyl group on the monolignol dimer. The opportunity for association between a molecule and an enzyme increases as the number of phenolic hydroxyl groups on the substrate increases. Therefore, one reason that the consumption rate of **III** was higher than those of **I** and **II** is the difference in the number of phenolic hydroxyl group present.

The reactions involving HRP and monolignol dimers may not be accurately represented by Michaelis–Menten kinetics, because the reaction products can act as substrates. We assumed that the early stage of these reactions were second-order to estimate the kinetics of monolignol dimers in enzymatic dehydrogenative polymerization. In a second-order reaction, the rate equation is represented by Eq. (2).

$$-\frac{\mathrm{d}[A]}{\mathrm{d}t} = k[A]^2 \tag{2}$$

where $[A]$ is the concentration of the substrate (mmol/L), t is time (min), and k is the rate constant.

The rate constants (k) for the early stage of the single-component reactions (reaction time: 0–3 min) for **CA**, **I**, **II**, and **III**, calculated by Eq. (2), were 202, 0.63, 3.2 and 7.5, respectively. The rate constant for **I** was 20 % of that of **II**, and that of **III** was 234 % of that for **II**. Pinoresinol monomethyl ether (Fig. 1, **IV**) was synthesized to estimate the effect of the number of phenolic hydroxyl groups on the consumption rate for the single-component reaction. The rate constant for **IV** was 84 % of that of **II**. Therefore, the rate constant for **III** was nearly twice that of **II** and **IV**. These results tell us that the number of phenolic hydroxyl groups present on monolignol dimers have an effect on their reaction rates.

However, the result that the consumption rate of **I** was much lower than those of **II** and **IV** cannot be explained by this rationale, since the number of phenolic hydroxyl groups on these molecules is the same. As another factor affecting the consumption rates of the oxidation of monolignol dimers was thought to be the oxidation potentials, the monolignol dimers were subjected to CV analysis. The results showed that the oxidation potential of the phenolic hydroxyl group on different monolignol dimers have similar values. Therefore, the difference in the consumption rates among the dimers must be due to another factor, such as the substrate specificity of the enzyme. Recall that, in this study, we used HRP as the enzyme for dehydrogenative polymerization. It was previously reported that HRP and *Arabidopsis thaliana* peroxidase A2, which is 95 % identical to HRP A2, catalyzes the dehydrogenative polymerization of **CA**, although this enzyme did not efficiently polymerize sinapyl alcohol, probably due to steric hindrance [26, 27]. Steric hindrance between substrates and HRP was not only due to amino acid residue on the entrance to the active site, but was also due to the molecular volume of the substrate [28]. In the case of sinapyl alcohol, steric hindrance occurs between the methoxy group of sinapyl alcohol and the backbone atoms of Ile138 and Pro139 residues which are located in the active site of HRP and other plant peroxidases belonging to class III peroxidase [26, 27]. These findings were obtained in studies conducted on monolignols, not monolignol dimers. However, they are useful for the discussion of the oxidation activity of HRP with both monolignol dimers and oligomers. Earlier in this paragraph, it was suggested that the substrate specificity of HRP is related to the steric structure of the substrate. The steric structures of the three monolignol dimers used in this study in aqueous solution are different. Therefore, their accessibilities to the enzyme should also be different. This difference probably affected the consumption rate of each monolignol dimer.

Consumption rates of monolignol dimers in mixed-component reactions

The quantity of enzyme and substrate in each mixed-component reaction were the same as those in the single-component reactions. Therefore, the contact frequency between the substrate and the enzyme should be the same in all reaction systems, and the consumption rates of the dimers in the mixed-component reactions should be the same as those in the single-component reactions. However, the consumption rates of the dimers in the mixed-component reactions were different from those in the single-component reactions. Furthermore, the consumption rates of the dimers changed in both directions at the same time. Therefore, it is reasonable to hypothesize that another mechanism is responsible for the increase and decrease in the consumption rates of the dimers in mixed-component reactions. One possible mechanism is that radical mediation occurs in the mixed-component reactions of monolignol dimers. Radical mediation has been reported previously in some reactions of phenolic compounds in various mixed-component reaction systems. It was reported that sinapyl alcohol can be oxidized by peroxidases with a low reactivity for sinapyl alcohol in the presence of other phenolic compounds such as hydroxycinnamic acids and **CA**, as these phenolic compounds act as radical mediators [15, 29–31]. It was also reported that a large molecular weight compound, such as chlorogenic acid is capable of acting as a radical mediator in HRP-catalyzed reactions [32]. Therefore, radical mediation in HRP-catalyzed dehydrogenative polymerization of the **CA** dimers should be possible.

The CV analysis shows that the oxidation potentials of all monolignol dimers used in this study were almost identical. Therefore, radical transfer probably occurs in

both directions. From the results of the mixed-component reaction of **I** + **II** and **I** + **III**, it is evident that radical transfer occurs mainly from **II** and **III** to **I**. A possible mechanism in which both **II** and **III** act as radical mediators in the mixed-component reaction with **I** is shown in Fig. 7. When **II** or **III** works as a radical mediator, the free radical of **II** or **III** generated by HRP withdraws a single electron from **I**, generating a free radical adduct of **I**. In such a radical mediation system, the apparent consumption rate of **II** or **III** decreases while that of **I** increases in mixed-component reactions compared with single-component reactions.

Radical transfer occurs when a phenolic hydroxyl group in a dimer contacts another dimer radical. In **I** + **II** and **I** + **III**, the quantity of phenolic hydroxyl groups in **I** is higher than in **II** or **III** because the consumption rate of **I** was lower than that of **II** or **III**. Therefore, it was easier for **II** and **III** radicals to contact phenolic hydroxyl groups in **I**, leading to the preferential transfer of an electron from the **II** or **III** radical to **I**.

Although the reaction rate of **III** is higher than that of **II**, radical transfer mainly occurred from **II** to **III** in the mixed-component reaction of **II** + **III**. This is probably because the abundance of hydroxyl groups in **III** was higher than that of **II**.

Qualitative analyses of reaction products

Free radicals generated at the phenolic hydroxyl group (C-4-OH) of a monolignol can be transferred to C-1, C-5, or C-β [33], and the radical coupling reactions conducted to produce monolignol dimers result mainly in the generation of **I**, **II**, and **III** [34]. In the same manner, radical coupling reactions between **I**, **II**, and **III** may occur via radicals at C-4-O and C-5 to form 5-*O*-4 or 5-5 linkages. Indeed, linkages between some of the monolignol tetramers present in the reaction products were identified as being constructed by 5-*O*-4 and 5-5 linkages. This result is consistent with previous reports about linkages among monolignol dimers and oligomers [35, 36]. In LC–MS chromatograms of all single-component reaction products, shown in Figs. 4a, 5a, and 6a, major peaks for monolignol tetramers with 5-*O*-4 and 5-5 linkages were recorded. Some previous studies on computer simulations of electron densities and electron paramagnetic resonances suggested that **II** was hardly oxidized by peroxidase [37, 38]. However, in the

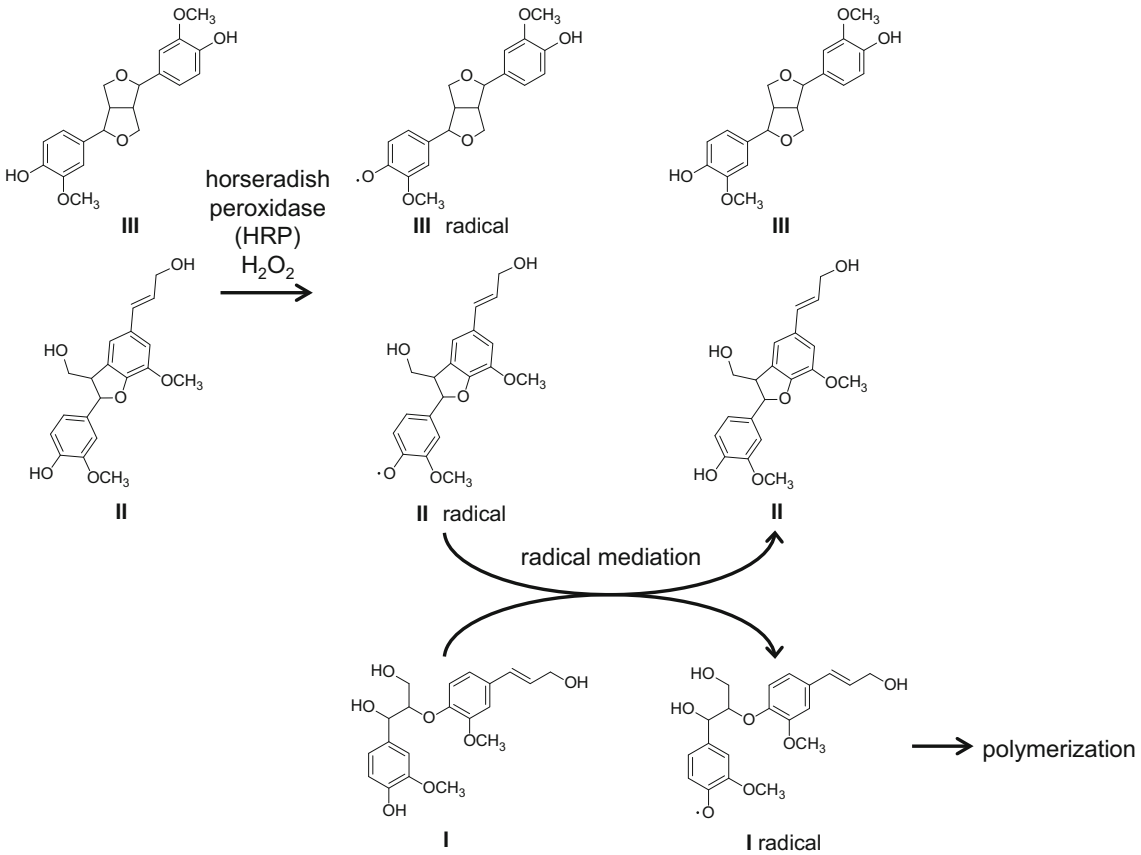

Fig. 7 Conceivable mechanism of **II** or **III** as a radical mediator in the mixed-component reaction with **I**. Generated **II** or **III** radical withdraws a single electron from **I**. Then, free radical adduct of **I** is generated while **II** or **III** turns back to its original state

current work, it has been shown that **II** does participate in the dehydrogenative polymerization catalyzed by HRP, leading to the production of monolignol oligomers.

This study is the first step in the clarification of the polymerization of monolignol dimers. Additional analyses are necessary for a complete understanding of HRP-catalyzed oxidation. In this study, HRP was used as the enzyme for the catalysis of dehydrogenative polymerization of monolignol dimers. As described in the introduction, HRP has been used as the primary enzyme in the study of lignification. In this study, we also used HRP as a model enzyme to find new insights into the early stage of lignin polymerization. However, HRP actually does not work for lignification in vivo. In the future, we would like to conduct additional studies using enzymes that have functionality in natural lignification, so that an understanding of the mechanism of the action of monolignol dimers and oligomers in lignification of plant cell walls can be gained.

Conclusion

Monolignol dimers **I**, **II**, and **III** derived from **CA**s were oxidized in the presence of HRP and H_2O_2, resulting in the formation of monolignol oligomers by radical coupling reactions. There was a significant difference in the consumption rates of these dimers. The consumption rate of **III** was the highest among the three dimers. One of the causes of this result is likely that **III** contains twice the number of phenolic hydroxyl groups as **I** and **II**. There was very little difference in the oxidation potentials measured for the dimers, which implied that the reaction rate of the dimers was not related to the oxidation potential. After conducting the reaction for 3 h, both the single-component and mixed-component reactions produced monolignol tetramers and hexamers derived from the monolignol dimers, as detected by LC–MS analyses. Furthermore, monolignol octamers were detected in the products of the reaction systems containing **II**. The monolignol tetramers were identified in the products of single-component reaction systems, and were shown by MS analysis to be formed by 5-5 and 5-*O*-4 couplings between the monolignol dimer units. HRP-catalyzed oxidation reactions utilizing a mixture of dimers indicated that monolignol dimers can function as radical mediators. In plant cell wall biosynthesis, cellulose and hemicellulose are synthesized first, and then the cell walls are lignified [39–41]. The reaction mechanism that proceeds via radical mediation is thought to be an effective and efficient process by which lignification can occur in the narrow space between polysaccharides.

References

1. Boerjan W, Ralph J, Baucher M (2003) Lignin biosynthesis. Annu Rev Plant Biol 54:519–546
2. Hepler PK, Fosket DE, Newcomb EH (1970) Lignification during secondary wall formation in coleus: an electron microscopic study. Amer J Bot 57:85–96
3. Åkerholm M, Salmén L (2003) The Oriented structure of lignin and its viscoelastic properties studied by static and dynamic FT-IR spectroscopy. Holzforschung 57:459–465
4. Peura M, Grotkopp I, Lemke H, Vikkula A, Laine J, Müller M, Serimaa R (2006) Negative poisson ratio of crystalline cellulose in kraft cooked Norway spruce. Biomacromolecules 7:1521–1528
5. Stevanic JS, Salmén L (2009) Orientation of the wood polymers in the cell wall of spruce wood fibres. Holzforschung 63:497–503
6. Ride JP (1975) Lignification in wounded wheat leaves in response to fungi and its possible role in resistance. Physiol Plant Pathol 5(2):125–134
7. Vance CP, Kirk TK, Sherwood RT (1980) Lignification as a mechanism of disease resistance. Ann Rev Phytopathol 18:259–288
8. Cheong YH, Chang HS, Gupta R, Wang X, Zhu T, Luan S (2002) Transcriptional profiling reveals novel interactions between wounding, pathogen, abiotic stress, and hormonal responses in *Arabidopsis*. Plant Physiol 129(2):661–677
9. Freudenberg K (1959) Biosynthesis and constitution of lignin. Nature 183:1152–1155
10. Takahama U (1995) Oxidation of hydroxycinnamic acid and hydroxycinnamyl alcohol derivatives by laccase and peroxidase. Interactions among *p*-hydroxyphenyl, guaiacyl and syringyl groups during the oxidation reactions. Physiol Plant 93:61–68
11. Ros Barceló A (1997) Lignification in plant cell walls. Int Rev Cytol 176:87–132
12. Blinkovsky AM, Dordick JS (1993) Peroxidase-catalyzed synthesis of lignin–phenol copolymers. J Polym Sci Part A Polym Chem 31:1839–1846
13. van Parijs FRD, Morreel K, Ralph J, Boerjan W, Merks RMH (2010) Modeling lignin polymerization. I. Simulation model of dehydrogenation polymers. Plant Physiol 153:1332–1344
14. Wang C, Qian C, Roman M, Glasser WG, Esker AR (2013) Surface-initiated dehydrogenative polymerization of monolignols: a quartz crystal microbalance with dissipation monitoring and atomic force microscopy study. Biomacromolecules 14:3964–3972
15. Fournand D, Cathala B, Lapierre C (2003) Initial steps of the peroxidase-catalyzed polymerization of coniferyl alcohol and/or sinapyl aldehyde: capillary zone electrophoresis study of pH effect. Phytochemistry 62(2):139–146
16. Demont-Caulet N, Lapierre C, Jouanin L, Baumberger S, Méchin V (2010) *Arabidopsis* peroxidase-catalyzed copolymerization of coniferyl and sinapyl alcohols: kinetics of an endwise process. Phytochemistry 71:1673–1683
17. Grabber JH, Hatfirld RD, Ralph J (2003) Apoplastic pH and monolignol addition rate effects on lignin formation and cell wall degradability in maize. J Agric Food Chem 51:4984–4989
18. Barakat A, Winter H, Rondeau-Mouro C, Saake B, Chabbert B, Cathala B (2007) Studies of xylan interactions and cross-linking to synthetic lignins formed by bulk and end-wise polymerization: a model study of lignin carbohydrate complex formation. Planta 225:267–281
19. Adler E (1977) Lignin chemistry–past, present and future. Wood Sci Technol 11(3):169–218
20. Ralph J, Lundquist K, Brunow G, Lu F, Kim H, Schatz PF, Marita JM, Hatfield RD, Ralph SA, Christensen JH, Boerjan W (2004) Lignins: natural polymers from oxidative coupling of 4-hydroxyphenyl-propanoids. Phytochem Rev 3:29–60

21. Freudenberg K, Hübner HH (1952) Hydroxy cinnamyl alcohols and their dehydrogenative polymerization (in German). Chem Ber 85:1181–1191
22. Sangha AK, Parks JM, Standaert RF, Ziebell A, Davis M, Smith JC (2012) Radical coupling reactions in lignin synthesis: a density functional theory study. J Phys Chem B 116:4760–4768
23. Terashima N, Tomimura Y, Arai H (1979) Heterogeneity in formation of lignin. III. Formation of condensed type structure with bond at position 5 of guaiacyl nucleus. Mokuzai Gakkaishi 25:595–599
24. Quideau S, Ralph J (1994) A biomimetic route to lignin model compounds via silver (I) oxide oxidation. Holzforschung 48:12–22
25. Fergus BJ, Goring DAI (1970) The location of guaiacyl and syringyl lignins in birch xylem tissue. Holzforschung 24(4):113–117
26. Østergaard L, Teilum K, Mirza O, Mattsson O, Petersen M, Welinder KG, Mundy J, Gajhede M, Henriksen A (2000) *Arabidopsis* ATP A2 peroxidase. Expression and high-resolution structure of a plant peroxidase with implications for lignification. Plant Mol Biol 44:231–243
27. Nielsen KL, Indiani C, Henriksen A, Feis A, Becucci M, Gajhede M, Smulevich G, Welinder KG (2001) Differential activity and structure of highly similar peroxidases. Spectroscopic, crystallographic, and enzymatic analyses of lignifying *Arabidopsis thaliana* peroxidase A2 and horseradish peroxidase A2. Biochemistry 40:11013–11021
28. Kobayashi T, Taguchi H, Shigematsu M, Tanahashi M (2005) Substituent effects of 3,5-disubstituted *p*-coumaryl alcohol on their oxidation using horseradish peroxidase–H_2O_2 as the oxidant. J Wood Sci 51:607–614
29. Takahama U, Oniki T, Shimokawa H (1996) A possible mechanism for the oxidation of sinapyl alcohol by peroxidase-dependent reactions in the apoplast: enhancement of the oxidation by hydroxycinnamic acids and components of the apoplast. Plant Cell Physiol 37(4):499–504
30. Takahama U, Oniki T (1997) Enhancement of peroxidase-dependent oxidation of sinapyl alcohol by an apoplastic component, 4-coumaric acid ester isolated from epicotyls of *Vigna angularis* L. Plant Cell Physiol 38(4):456–462
31. Aoyama W, Sasaki S, Matsumura S, Mitsunaga T, Hirai H, Tsutsumi Y, Nishida T (2002) Sinapyl alcohol-specific peroxidase isoenzyme catalyzes the formation of the dehydrogenative polymer from sinapyl alcohol. J Wood Sci 48:497–504
32. Yamasaki H, Grace SC (1998) EPR detection of phytophenoxyl radicals stabilized by zinc ions: evidence for the redox coupling of plant phenolics with ascorbate in the H_2O_2-peroxidase system. FEBS Lett 422:377–380
33. Shigematsu M, Masamoto H (2008) Solvent effects on the electronic state of monolignol radicals as predicted by molecular orbital calculations. J Wood Sci 54:308–311
34. Shigematsu M, Kobayashi T, Taguchi H, Tanahashi M (2006) Transition state leading to β-O' quinonemethide intermediate of *p*-coumaryl alcohol analyzed by semi-empirical molecular orbital calculation. J Wood Sci 52:128–133
35. Önnerud H (2003) Lignin structures in normal and compression wood. Evaluation by thioacidolysis using ethanethiol and methanethiol. Holzforschung 57:377–384
36. Yue F, Lu F, Sun R, Ralph J (2012) Synthesis and characterization of new 5-linked pinoresinol lignin models. Chem Eur J 18:16402–16410
37. Sangha AK, Davison BH, Standaert RF, Davis MF, Smith JC, Parks JM (2014) Chemical factors that control lignin polymerization. J Phys Chem B 118:164–170
38. Russell WR, Burkitt MJ, Scobbie L, Chesson A (2006) EPR investigation into the effects of substrate structure on peroxidase-catalyzed phenylpropanoid oxidation. Biomacromolecules 7:268–273
39. Takabe K, Fujita M, Harada H, Saiki H (1981) Lignification process of Japanese black pine (*Pinus thunbergii* Parl.) tracheids. Mokuzai Gakkaishi 27:813–820
40. Terashima N, Fukushima K (1988) Heterogeneity in formation of lignin–XI: an autoradiographic study of the heterogeneous formation and structure of pine lignin. Wood Sci Technol 22:259–270
41. Fukushima K, Terashima N (1991) Heterogeneity in formation of lignin XIV. Formation and structure of lignin in differentiating xylem of *Ginkgo biloba*. Holzforschung 45:87–94